Dynamics and mechanics of motor-filament systems

K. Kruse[a] and F. Jülicher

Max-Planck-Institut für Physik komplexer Systeme, Nöthnitzerstr. 38, 01187 Dresden, Germany

Abstract. Motivated by the cytoskeleton of eukaryotic cells, we develop a general framework for describing the large-scale dynamics of an active filament network. In the cytoskeleton, active cross-links are formed by motor proteins that are able to induce relative motion between filaments. Starting from pair-wise interactions of filaments via such active processes, our framework is based on momentum conservation and an analysis of the momentum flux. This allows us to calculate the stresses in the filament network generated by the action of motor proteins. We derive effective theories for the filament dynamics which can be related to continuum theories of active polar gels. As an example, we discuss the stability of homogenous isotropic filament distributions in two spatial dimensions.

PACS. 87.16.Ka Filaments, microtubules, their networks, and supramolecular assemblies – 87.16.Nn Motor proteins (myosin, kinesin dynein) – 87.16.-b Subcellular structure and processes

1 Introduction

The cytoskeleton is a subsystem of living cells that plays an essential role in various cellular processes such as cell locomotion and cell division [1–3]. The principal components of the cytoskeleton are actin and tubulin. These proteins can aggregate into filamentous structures, respectively called actin-filaments and microtubules. The two filament ends have different properties and define an orientation for a filament that can be characterized by a vector. Interactions with a large number of proteins make the network of actin-filaments and microtubules highly dynamic. There are proteins that nucleate filaments, regulate their lengths in various ways, and form cross-links between filament pairs. Many of these processes involve the release of chemical energy during the hydrolysis of nucleotide triphosphates, in particular adenosine tri-phosphate (ATP). In a living cell, differences in the chemical potentials of ATP and its hydrolysis products are maintained, which keeps the cytoskeleton out of thermodynamic equilibrium. The hydrolysis of ATP drives in particular motor proteins, *e.g.*, myosins or kinesins. These molecules can use the filaments as tracks along which they transport cargo into a direction that is determined by the filament's orientation. Connecting two filaments, motor proteins or complexes thereof can induce relative displacements of the two filaments and generate stresses in the filament network.

Summarizing these features from a physical point of view, the cytoskeleton is an example of an active polar gel [4]. In recent years phenomenological continuum theories describing various aspects of the dynamics of active polar gels have been developed [4–11]. Using these descriptions, the dynamics of filament networks has been studied in different situations such as topological point defects [4–6,9,10] as well as the formation of contractile rings [11].

Experimental works on active polar gels outside living cells have focused on purified systems containing filaments and a few associated proteins [12–18]. In particular, collective effects in motor-filament systems were studied. Through the action of motors, bundles of filaments were found to contract and to separate filaments according to their polarity [12,18]. In two dimensions, initially homogenous isotropic distributions of filaments formed vortices and asters as the motor density was increased [13,14,16]. These experiments called for more microscopic descriptions of filament-motor systems. Such descriptions were applied to study the dynamics of bundles of motors and filaments as well as the stability of homogenous isotropic distributions and the formation of asters in two dimensions [13,16,19–27].

A general framework for the description of the dynamics of bundles of polar filaments induced by active cross-linkers based on microscopic rules for the interaction of filament pairs via active cross-linkers was presented in reference [22]. This framework is based on the momentum balance in the system and can describe the stresses generated. In the present work we extend this formalism to higher dimensions. Expression for the currents of filaments

---

[a] *Present address*: Institut für Theoretische Physik, Universität des Saarlandes, Postfach 15 11 50, 66041 Saarbrücken, Germany; e-mail: `karsten@lusi.uni-sb.de`

and motors will be introduced in Section 2. In Section 3, the stresses in the system are expressed in terms of the forces exerted by motors. As an example, we apply the formalism to study the stability of two-dimensional isotropic homogenous filament distributions in the presence of motor proteins in Section 4.

2 Forces and currents

We describe the system consisting of polar filaments and motors by the filament density Ψ and the densities m_b of bound and m_u of unbound motors. The filaments are taken to be thin, rigid rods, such that filament bending and rotation around the rod axis can be ignored. The function $\Psi(\mathbf{x}, \mathbf{u})$ denotes the density of filaments with their center at position $\mathbf{x}$ having an orientation described by the unit vector $\mathbf{u}$ with $\mathbf{u}^2 = 1$. For simplicity, we assume that the distribution of the filament lengths is the same for all points in space and that it is constant in time. Motors are assumed to be small as compared to the linear extension of the filaments and are therefore treated as point particles. We will focus on the case of only one motor species, but the extension to several species possibly moving into different directions on a filament is straightforward.

The time evolution of the filament and motor densities can be written in the form of continuity equations,

$$\partial_t \Psi - \nabla \cdot \left[D_\parallel \mathbf{u}\mathbf{u} + D_\perp (1 - \mathbf{u}\mathbf{u}) \right] \cdot \nabla \Psi$$
$$- D_r \boldsymbol{\mathcal{R}} \cdot \boldsymbol{\mathcal{R}} \Psi + \nabla \cdot \mathbf{J}_a + \boldsymbol{\mathcal{R}} \cdot \mathbf{J}_r = S, \qquad (1)$$

$$\partial_t m_b - D_\mathrm{b} \Delta m_b + \nabla \cdot \mathbf{J}_\mathrm{b} = S_\mathrm{m}, \qquad (2)$$

$$\partial_t m_u - D_u \Delta m_u = -S_m, \qquad (3)$$

where $\boldsymbol{\mathcal{R}} = \mathbf{u} \times \partial/\partial\mathbf{u}$ is the rotation operator. The parameters $D_\parallel$, $D_\perp$, D_r, and D_b are effective diffusion constants and account for fluctuations in the system. They, respectively, describe fluctuations in the position of filaments along and perpendicular to their axis, fluctuations in the filament orientation [28], as well as fluctuations in the position of bound motors. A major source for fluctuations is the randomness inherent in the motor-filament interactions. This implies in particular, that the effective diffusion constants do not fulfill the Einstein relation. In contrast, unbound motors are assumed to simply diffuse thermally with diffusion constant D_u. The translational and the rotational filament currents, $\mathbf{J}_a$ and $\mathbf{J}_r$, as well as the motor current $\mathbf{J}_b$ are generated by active interactions between motors and filaments and will be specified below. Finally, we have introduced the source terms S and S_m. They, respectively, capture the effects of nucleation and disappearance of filaments as well as the exchange of motors bound to filaments for unbound motors in the surrounding fluid. Note, that we have neglected excluded-volume effects, which can be included in a standard way [23,26,28].

We will now derive explicit expressions for the active filament and motor currents for the special situation where filaments slide relative to each other in a resting fluid. This situation corresponds in particular to a filament network close to a solid surface or the cell cortex in cells. We consider the flux of momentum in the system. Momentum
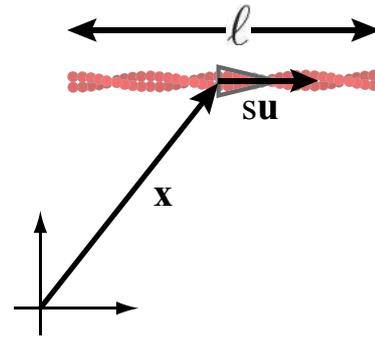
Fig. 1. Illustration of the quantities used to characterize the position and orientation of a filament. The filament's center is located at a point $\mathbf{x}$, its orientation given by $\mathbf{u}$ with $\mathbf{u}^2 = 1$. The length of the filament is ℓ and s is a linear coordinate along the filament with $s = 0$ in the center and with s increasing in the direction of $\mathbf{u}$.
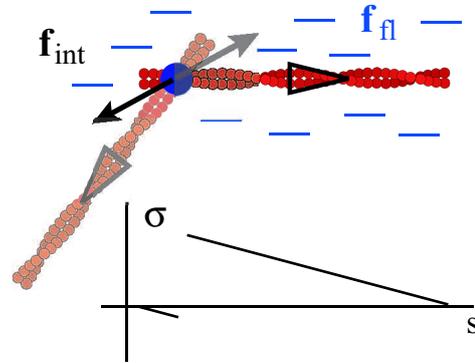
Fig. 2. Illustration of the forces acting on a filament. The (blue on-line) dot indicates a motor that cross-links the filaments to another and exerts a force. The density of these forces is denoted by $\mathbf{f}_\mathrm{int}$. The filament moves in a solvent represented by the horizontal lines, which results in friction forces $\mathbf{f}_\mathrm{fl}$. Due to these forces, a line tension σ builds up in the filament as indicated in the graph. For simplicity, external forces and friction forces of motors connected to a single filament are not indicated.

conservation corresponds to the conditions of force balance at each point $\mathbf{x} + s\mathbf{u}$ along every filament. Here, s is a linear coordinate along a filament which is zero in the center and increases in the direction of $\mathbf{u}$, see Figure 1. The forces acting on a filament create stresses in the filament that can be expressed as a line tension σ. The line tension has units of a force.

The forces acting on a filament are generated by motor proteins, result from friction with the surrounding solvent, or are external forces applied to the system, see Figure 2 for an illustration. As a result, the force balance at each point along a filament can be expressed as

$$\mathbf{u}\partial_s \sigma(\mathbf{x}, \mathbf{u}, s) - \mathbf{f}_\mathrm{int}(\mathbf{x}, \mathbf{u}, s) = \mathbf{f}_\mathrm{fl}(\mathbf{x}, \mathbf{u}, s) + \mathbf{f}_\mathrm{m}(\mathbf{x}, \mathbf{u}, s)$$
$$+ \mathbf{f}_\mathrm{ext}(\mathbf{x}, \mathbf{u}, s). \qquad (4)$$

Here, the density of internal forces is denoted by $\mathbf{f}_\mathrm{int}$ and describes the forces generated by motor proteins cross-linking filaments. The action of motors moving on a single

filament generates friction forces of density $\mathbf{f}_m$. Forces resulting from friction of the filaments with the surrounding fluid are captured by the density $\mathbf{f}_{fl}$. Finally, the density of external forces is denoted by $\mathbf{f}_{ext}$.

We start our discussion of the force densities with the friction forces. We will assume friction to be local, which is the case for an immobile solvent. Then friction forces along a filament depend only on the motion of this filament. The density of friction forces is thus related to the filament currents by

$$\mathbf{f}_{fl}(\mathbf{x}, \mathbf{u}, s) = \left[\eta_\parallel \mathbf{u}\mathbf{u} + \eta_\perp(1 - \mathbf{u}\mathbf{u})\right] \cdot \mathbf{J}_a(\mathbf{x}, \mathbf{u})R(s) \\ -\eta_0 s\mathbf{u} \times \mathbf{J}_r(\mathbf{x}, \mathbf{u})R(s). \quad (5)$$

Here, $\eta_\parallel$ and $\eta_\perp$ are friction coefficients per unit length for motion in the direction longitudinal and perpendicular to the filament axis, respectively. The coefficient η_0 describes the friction of a filament subunit, see [28]. Finally, the function R describes dissipation along the filament and reflects the distribution of filament lengths. In the case when all filaments are of the same length ℓ, a simple choice is $R(s) = 1$ for $|s| \leq \ell/2$ and $R(s) = 0$ otherwise.

Equation (5) can be used to express the active translational and rotational currents, $\mathbf{J}_a$ and $\mathbf{J}_r$, in terms of the internal, the motor and the external force densities. We will illustrate this in the case of no external forces and neglecting the force density of motors connected to single filaments. Since the friction of motors is very small as compared to the filament friction, the contribution of the latter to the filament current is indeed negligible. This is, however, no longer true if these motors transport large cargos[1]. For $\mathbf{f}_{ext} = 0$ and $\mathbf{f}_m = 0$, integration of equation (4) with respect to s yields

$$-\int ds\, \mathbf{f}_{int}(\mathbf{x}, \mathbf{u}, s) = \int ds\, \mathbf{f}_{fl}(\mathbf{x}, \mathbf{u}, s) \quad (6)$$

$$= \ell\left[\eta_\parallel \mathbf{u}\mathbf{u} + \eta_\perp(1 - \mathbf{u}\mathbf{u})\right] \cdot \mathbf{J}_a(\mathbf{x}, \mathbf{u}). \quad (7)$$

Here $\ell = \int ds\, R(s)$ and we have used $R(s) = R(-s)$. Therefore,

$$\mathbf{J}_a(\mathbf{x}, \mathbf{u}) = -\frac{1}{\ell}\left[\frac{1}{\eta_\parallel}\mathbf{u}\mathbf{u} + \frac{1}{\eta_\perp}(1 - \mathbf{u}\mathbf{u})\right] \cdot \int ds\, \mathbf{f}_{int}(\mathbf{x}, \mathbf{u}, s). \quad (8)$$

Integrating equation (4) as $\int ds\, s\mathbf{u}\times$ yields

$$\mathbf{J}_r(\mathbf{x}, \mathbf{u}) = -\frac{1}{\eta_0\chi^2}\int ds\, s\mathbf{u} \times \mathbf{f}_{int}(\mathbf{x}, \mathbf{u}, s). \quad (9)$$

Here, we have introduced $\chi^2 = \int ds\, s^2 R(s)$ and used $\mathbf{J}_r(\mathbf{x}, \mathbf{u}) \perp \mathbf{u}$. It is important to note that the rotational current is thus not independent of the translational current. Consequently, the description of the dynamics of active motor-filament systems is completed by specifying the internal force density $\mathbf{f}_{int}$. This density sums up all the forces exerted by motors connecting two or more filaments and hence depends on the filament and motor densities.

---

[1] If the density $\mathbf{f}_m$ is taken into account, then the friction of motors $\eta_m\mathbf{J}_m$, where η_m is an effective friction coefficient of a motor, must be added in equation (5).
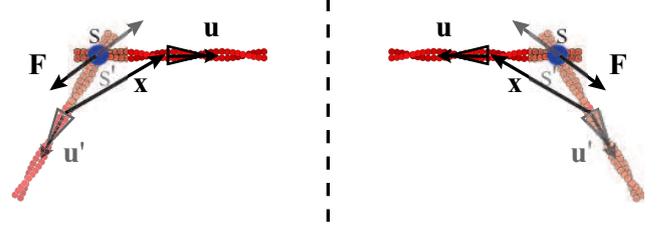
Fig. 3. Illustration of the constraints imposed on the force $\mathbf{F}$ exerted by an active cross-link on a filament. Left: original configuration. Translation of the filament pair does not change $\mathbf{F}$ implying equation (11). Rotation of the filament pair implies rotation of the vector $\mathbf{F}$ by the same angle, yielding condition (12). Right: the same filament pair after reflection with respect to the vertical dashed line implying conditions (13) and (14).

In the following we will assume that the dominant contribution to the internal forces results from interactions between filament pairs. We assume that filaments are cross-linked by motors only when they have an overlap. The force exerted by motors on a filament pair depends on the relative orientation and separation of filaments [20, 24, 25]. The density of internal forces acting at a point s on a filament with center at $\mathbf{x}$ and orientation $\mathbf{u}$ can then be expressed as

$$\mathbf{f}_{int}(\mathbf{x}, \mathbf{u}, s) = \int d\mathbf{x}' \int d\mathbf{u}' \int ds'\, \Psi(\mathbf{x}, \mathbf{u})\Psi(\mathbf{x}', \mathbf{u}')C_{\mathbf{x}, \mathbf{u}, s}^{\mathbf{x}', \mathbf{u}', s'} \\ \times m(\mathbf{x} + s\mathbf{u})\mathbf{F}(\mathbf{x}, \mathbf{u}, s, \mathbf{x}', \mathbf{u}', s'). \quad (10)$$

In this expression $C_{\mathbf{x}, \mathbf{u}, s}^{\mathbf{x}', \mathbf{u}', s'} = R(s)R(s')\delta(\mathbf{x} + s\mathbf{u} - \mathbf{x}' - s'\mathbf{u}')$ restricts the integration to those filaments that cross each other.

The function $\mathbf{F}$ denotes the average force between two filaments at the specified locations and orientations. It has to satisfy several constraints imposed by symmetry, as illustrated in Figure 3. We will assume in the following that the internal forces between filament pairs are covariant under translations, rotations and reflections. Due to translation invariance, $\mathbf{F}$ can only depend on relative positions of the filament centers

$$\mathbf{F}(\mathbf{x}, \mathbf{u}, s, \mathbf{x}', \mathbf{u}', s') \equiv \mathbf{F}(\mathbf{x} - \mathbf{x}', \mathbf{u}, s, \mathbf{u}', s'). \quad (11)$$

Covariance under rotations imposes

$$\mathbf{F}(\mathbf{R}(\varphi)\mathbf{x}, \mathbf{R}(\varphi)\mathbf{u}, s, \mathbf{R}(\varphi)\mathbf{u}', s') = \mathbf{R}(\varphi)\mathbf{F}(\mathbf{x}, \mathbf{u}, s, \mathbf{u}', s'), \quad (12)$$

for any φ, where $\mathbf{R}(\varphi)$ denotes the rotation operator for a rotation by an angle φ. Furthermore, covariance with respect to reflections requires

$$\mathbf{F}_\parallel(\mathbf{x}_\parallel + \mathbf{x}_\perp, \mathbf{u}_\parallel + \mathbf{u}_\perp, s, \mathbf{u}'_\parallel + \mathbf{u}'_\perp, s') = \\ \mathbf{F}_\parallel(\mathbf{x}_\parallel - \mathbf{x}_\perp, \mathbf{u}_\parallel - \mathbf{u}_\perp, s, \mathbf{u}'_\parallel - \mathbf{u}'_\perp, s'), \quad (13)$$

$$\mathbf{F}_\perp(\mathbf{x}_\parallel + \mathbf{x}_\perp, \mathbf{u}_\parallel + \mathbf{u}_\perp, s, \mathbf{u}'_\parallel + \mathbf{u}'_\perp, s') = \\ -\mathbf{F}_\perp(\mathbf{x}_\parallel - \mathbf{x}_\perp, \mathbf{u}_\parallel - \mathbf{u}_\perp, s, \mathbf{u}'_\parallel - \mathbf{u}'_\perp, s'), \quad (14)$$

where the subscripts $\parallel$ and $\perp$ denote vector components along and perpendicular to the reflection axis, respectively. Finally, the principle of *actio = reactio* implies

$$\mathbf{F}(\mathbf{x}, \mathbf{u}, s, \mathbf{u}', s') = -\mathbf{F}(-\mathbf{x}, \mathbf{u}', s', \mathbf{u}, s). \quad (15)$$

For completeness, let us specify the force density of motors bound to one filament only. We take it to be proportional to the motor and the filament density and write

$$\mathbf{f}_{\mathrm{m}}(\mathbf{x}, \mathbf{u}, s) = \eta_{\mathrm{m}} \Gamma \mathbf{u} \, m_b(\mathbf{x} + s\mathbf{u}) \Psi(\mathbf{x}, \mathbf{u}) R(s). \quad (16)$$

Here, Γ is the average velocity of motors moving on a filament and η_{m} the motor friction coefficient. The coefficient Γ depends on the fraction of bound motors that do not cross-link filaments.

3 The stress tensor

The formalism developed in the previous section can be used to calculate the stresses generated in a motor-filament system. The total stress tensor Σ_{tot} is defined through the relation

$$\mathbf{f}_{\mathrm{ext}} = \boldsymbol{\nabla} \cdot \Sigma_{\mathrm{tot}}, \quad (17)$$

where $\mathbf{f}_{\mathrm{ext}}$ is the density of external forces. The total stress tensor can be split up into two parts, one accounting for the stress in the filament-motor network, Σ, the other accounting for the stress in the solvent surrounding the network, Σ_{fl}, *i.e.*

$$\Sigma_{\mathrm{tot}} = \Sigma + \Sigma_{\mathrm{fl}}. \quad (18)$$

As before, we will assume that the solvent is immobile such that the stress Σ_{fl} is merely due to the motion of the filaments and the motors with respect to the fluid.

The stress in the filament network at a point $\mathbf{y}$ can be obtained from the fact that the divergence of the corresponding stress tensor must equal the sum of the forces $\mathbf{u} \partial_s \sigma$ acting on all filaments overlapping with $\mathbf{y}$, *i.e.*, $\int d\mathbf{x} \int d\mathbf{u} \int ds \, \mathbf{u} \partial_s \sigma \delta(\mathbf{y} - \mathbf{x} - s\mathbf{u})$. Integrating once by parts we find

$$\Sigma_{\alpha\beta}(\mathbf{y}) = \int d\mathbf{x} \int d\mathbf{u} \int ds \, u_\alpha u_\beta \sigma(\mathbf{x}, \mathbf{u}, s) \delta(\mathbf{y} - \mathbf{x} - s\mathbf{u}). \quad (19)$$

This relation expresses the stress in the filament network through the line tension in the individual filaments. Note that the tensor Σ is symmetric by definition, indicating that line tensions along filaments cannot generate torques in the system.

The line tension σ in turn can be expressed in terms of the internal force density. Consider again the case $\mathbf{f}_{\mathrm{ext}} = 0$ and $\mathbf{f}_{\mathrm{m}} = 0$. Expressing the density of friction forces through the density of internal forces by inserting equations (8) and (9) in equation (5) we find using equation (4)

$$\mathbf{u} \partial_s \sigma(\mathbf{x}, \mathbf{u}, s) = \mathbf{f}_{\mathrm{int}}(\mathbf{x}, \mathbf{u}, s) - \frac{1}{\ell} \int ds' \, \mathbf{f}_{\mathrm{int}}(\mathbf{x}, \mathbf{u}, s') R(s)$$

$$- \frac{1}{\chi^2} (1 - \mathbf{u}\mathbf{u}) \cdot \int ds' \, ss' \mathbf{f}_{\mathrm{int}}(\mathbf{x}, \mathbf{u}, s') R(s). \quad (20)$$

The stress in the solvent is generated by two processes, filaments and motors that slide with respect to the fluid. If as before we neglect for simplicity the effects of the force $\mathbf{f}_{\mathrm{m}}$ of motors interacting with single filaments, we have

$$\boldsymbol{\nabla} \cdot \Sigma_{\mathrm{fl}}(\mathbf{y}) = - \int d\mathbf{x} \int d\mathbf{u} \int ds \, \mathbf{f}_{\mathrm{fl}}(\mathbf{x}, \mathbf{u}, s) \delta(\mathbf{y} - \mathbf{x} - s\mathbf{u}). \quad (21)$$

Using equation (5) one can write the force balance

$$\boldsymbol{\nabla} \cdot \Sigma_{\mathrm{fl}} = -\eta_\parallel \mathbf{j}_\parallel - \eta_\perp \mathbf{j}_\perp - \eta_0 \mathbf{j}_0. \quad (22)$$

Here, we have defined the mass currents parallel and perpendicular to the local filament orientation $\mathbf{j}_\parallel$ and $\mathbf{j}_\perp$, as well as the mass current resulting from filament rotations $\mathbf{j}_0$. They are given by

$$\mathbf{j}_\parallel(\mathbf{y}) = \int d\mathbf{x} \int d\mathbf{u} \int ds \, \mathbf{u}\mathbf{u} \cdot \mathbf{J}_a(\mathbf{x}, \mathbf{u}) R(s) \delta(\mathbf{y} - \mathbf{x} - s\mathbf{u}), \quad (23)$$

$$\mathbf{j}_\perp(\mathbf{y}) = \int d\mathbf{x} \int d\mathbf{u} \int ds \, (1 - \mathbf{u}\mathbf{u}) \cdot \mathbf{J}_a(\mathbf{x}, \mathbf{u}) R(s)$$
$$\times \delta(\mathbf{y} - \mathbf{x} - s\mathbf{u}), \quad (24)$$

$$\mathbf{j}_0(\mathbf{y}) = - \int d\mathbf{x} \int d\mathbf{u} \int ds \, s\mathbf{u} \times \mathbf{J}_r(\mathbf{x}, \mathbf{u}) R(s)$$
$$\times \delta(\mathbf{y} - \mathbf{x} - s\mathbf{u}). \quad (25)$$

The total mass current at $\mathbf{y}$ given by

$$\mathbf{j}(\mathbf{y}) = \int d\mathbf{x} \int d\mathbf{u} \int ds \, [\mathbf{J}_a(\mathbf{x}, \mathbf{u}) R(s)$$
$$- s\mathbf{u} \times \mathbf{J}_r(\mathbf{x}, \mathbf{u}) R(s)] \, \delta(\mathbf{y} - \mathbf{x} - s\mathbf{u}) \quad (26)$$

obeys $\mathbf{j} = \mathbf{j}_\parallel + \mathbf{j}_\perp + \mathbf{j}_0$.

In the absence of external forces, $\mathbf{f}_{\mathrm{ext}} = 0$, equations (17) and (18) imply $\boldsymbol{\nabla} \cdot \Sigma = -\boldsymbol{\nabla} \cdot \Sigma_{\mathrm{fl}}$. Using this together with equations (19) and (20), the total mass current can be expressed in terms of the internal force density. This relation bridges the gap between the more microscopic approach developed here and the phenomenological description of reference [8].

Note that while the stress which results from pair-wise filament interactions σ is always symmetric, Σ_{fl} can have in general an asymmetric part, in particular if $\mathbf{f}_{\mathrm{m}} \neq 0$. Such an asymmetric part corresponds to a net torque in the system and would occur in situations with rotating currents [10].

4 Coarse-grained description in 2 dimensions

On length scales large compared to the filament length, the filament dynamics and force generation described above can be captured by an effective local continuum description. This can be illustrated by specifying the internal forces in a simple example based on a two-dimensional geometry. Such a two-dimensional description is motivated by *in vitro* experiments with stabilized microtubules and kinesin motor complexes [13,16] and by the cell cortex [1, 11]. For simplicity, we set the source term S in equation (1)

equal to zero, which corresponds to the case of stabilized filaments. Furthermore, we suppose all filaments to be of the same length ℓ and choose $R(s) = 1$ for $|s| \leq \ell/2$ and 0 otherwise. In order to keep the discussion simple, we focus on the case of a homogenous motor distribution. It remains to fix the form of the local force density $\mathbf{F}$. The simple and elegant form introduced in [23]

$$\mathbf{F}(\mathbf{x}, \mathbf{u}, s, \mathbf{u}', s') = \frac{\alpha}{2} \frac{\mathbf{x}}{\ell} \frac{1 + \mathbf{u} \cdot \mathbf{u}'}{\sqrt{1 - \mathbf{u} \cdot \mathbf{u}'}} + \frac{\beta}{2} \frac{\mathbf{u}' - \mathbf{u}}{\sqrt{1 - \mathbf{u} \cdot \mathbf{u}'}}, \quad (27)$$

satisfies all symmetry requirements. Again for simplicity, we will consider in the following the case $\beta = 0$.

Putting everything together, the active translational and rotational currents $\mathbf{J}_a$ and $\mathbf{J}_r$ can be calculated. From these expressions the dynamics on large length scales are obtained by performing a moment and gradient expansion [23,26]. The moment expansion consists of replacing the full filament distribution Ψ by its moments with the first ones being the filament density $c(\mathbf{x}) = \int d\mathbf{u}\, \Psi(\mathbf{x}, \mathbf{u})$ and the average polarization $\mathbf{p}(\mathbf{x}) = \int d\mathbf{u}\, \mathbf{u}\Psi(\mathbf{x}, \mathbf{u})$. The next higher moment would involve the nematic order parameter [11], but we will focus in the following on the density and the polarization. From the gradient expansion we will only retain terms containing up to fourth-order derivatives. Then, all the integrals appearing in the current can be carried out and we are left with a system of coupled partial differential equations describing the dynamics. In order to study the effect of $\eta_\perp \neq \eta_\parallel$ we will now analyze the linear stability of the homogenous isotropic distribution. An analysis of the non-linear regime in the case $\eta_\perp = \eta_\parallel$ has been presented in reference [26].

The homogenous isotropic distribution with $c(\mathbf{x}) = c_0$ and $\mathbf{p}(\mathbf{x}) = \mathbf{0}$ is a stationary state. Linearization of the dynamic equations with respect to this state gives

$$\partial_t c = \frac{1}{2}(D_\parallel + D_\perp)\Delta c - \bar{\alpha}\left[\Delta c + \frac{19}{480}\ell^2 \Delta\Delta c\right]$$
$$- \bar{\alpha}\left(1 - \frac{\eta_\parallel}{\eta_\perp}\right)\left[\frac{3}{4}\Delta c + \frac{31}{960}\ell^2 \Delta\Delta c\right], \quad (28)$$

$$\partial_t \mathbf{p} = D_\perp \Delta\mathbf{p} + (D_\parallel - D_\perp)\left(\frac{1}{2}\boldsymbol{\nabla}(\boldsymbol{\nabla}\cdot\mathbf{p}) + \frac{1}{4}\Delta\mathbf{p}\right) - D_r\mathbf{p}$$
$$- \bar{\alpha}\left[\frac{1}{2}\boldsymbol{\nabla}(\boldsymbol{\nabla}\cdot\mathbf{p}) + \frac{1}{4}\Delta\mathbf{p} + \frac{1}{30}\ell^2\boldsymbol{\nabla}\Delta(\boldsymbol{\nabla}\cdot\mathbf{p}) + \frac{11}{1920}\ell^2\Delta\Delta\mathbf{p}\right]$$
$$- \bar{\alpha}\left(1 - \frac{\eta_\parallel}{\eta_\perp}\right)\left[\frac{1}{2}\boldsymbol{\nabla}(\boldsymbol{\nabla}\cdot\mathbf{p}) + \frac{3}{16}\Delta\mathbf{p} + \frac{1}{32}\ell^2\boldsymbol{\nabla}\Delta(\boldsymbol{\nabla}\cdot\mathbf{p})\right.$$
$$\left. + \frac{13}{3840}\ell^2\Delta\Delta\mathbf{p}\right], \quad (29)$$

where $\bar{\alpha} = \alpha\ell^2 c_0/(24\eta_\parallel)$. In linear order, the dynamics of the density thus decouples from the dynamics of the polarization vector.

We will now analyze the stability of the homogenous isotropic state with respect to perturbations in the density and the polarization. Perturbations in the density will decay as long as the interaction strength α is below a critical

value α_c with

$$\alpha_c = \frac{48\eta_\perp\eta_\parallel}{7\eta_\perp - 3\eta_\parallel}\frac{D_\parallel + D_\perp}{c_0\ell^2}. \quad (30)$$

While qualitatively this critical value shows a similar dependence on the density c_0, the filament length ℓ and the diffusion constants $D_\parallel$ and $D_\perp$ as in one dimension, see [20], a new effect occurs due to differences between the longitudinal and transverse friction coefficients. For a bare microtubule or actin-filament one might expect $\eta_\parallel$ to be smaller than $\eta_\perp$. As these two values approach each other, the stability of the homogenous state increases. By adding appropriate proteins to the surface of a cytoskeletal filament, friction in the longitudinal direction might be larger than in the perpendicular direction[2]. If $\eta_\parallel$ exceeds $7\eta_\perp/3$, then fluctuations in the density will be unstable for negative values of α. These correspond to motors pushing filaments apart rather than pulling them together. Changing the relative values of longitudinal and perpendicular friction of the filaments thus provides the possibility of switching between different states of the system. Note that α_c is independent of the coefficient of rotational diffusion D_r.

There is also a critical value α_p such that perturbations in the polarization grow if $\alpha > \alpha_p$. The general expression for α_p is somewhat more complicated than the one for α_c and will not be given here. For the special case $D_r = 0$ we find

$$\alpha_p = \frac{96\eta_\perp\eta_\parallel}{23\eta_\perp - 11\eta_\parallel}\frac{D_\perp + 3D_\parallel}{c_0\ell^2}. \quad (31)$$

The corresponding unstable mode is a plane wave with the polarization longitudinal to the wave vector [23,26]. The transverse mode is always stable. Comparing α_c and α_p we see, that as long as $\eta_\parallel < 23\eta_\perp/11$ an instability of the homogenous isotropic state will occur first in the polarization. In the general case with $D_r \neq 0$, the instability occurs first in the density if the average density is below a certain critical value.

Finally, our analysis reveals that we can write the coarse-grained filament dynamics in the form [8,11]

$$\partial_t c = \nabla \cdot \mathbf{j}, \quad (32)$$
$$\partial_t \mathbf{p} = \boldsymbol{\omega}, \quad (33)$$

where the current $\mathbf{j}$ and the rate of change of the polarization $\boldsymbol{\omega}$ depend on the density c and orientation $\mathbf{p}$ of filaments. The force balance equation (21) of the microscopic theory suggests, that in the coarse-grained limit the current is related to the stresses by

$$\nabla \cdot \boldsymbol{\Sigma} = \eta \cdot \mathbf{j}, \quad (34)$$

where the mobility tensor is of the form

$$\eta = \eta_\parallel^{\text{eff}}\frac{\mathbf{pp}}{c^2} + \eta_\perp^{\text{eff}}\left(1 - \frac{\mathbf{pp}}{c^2}\right). \quad (35)$$

---

[2] MAP1 microtubule-binding proteins have arms sticking off the microtubule surface and might have this effect. Flagellates with mastigonemes, that are hair-like filaments on the flagella surface, swim in the direction of the wave propagating along the flagellum as a consequence of $\eta_\perp < \eta_\parallel$, see reference [29].

Note that coarse-graining of the microscopic currents defined in equations (23–25) leads to the parallel and perpendicular mass currents

$$\mathbf{j}_\parallel = \frac{\mathbf{pp}}{c^2} \cdot \mathbf{j}, \tag{36}$$

$$\mathbf{j}_\perp = \left(1 - \frac{\mathbf{pp}}{c^2}\right) \cdot \mathbf{j} \tag{37}$$

which contain rotational components and obey $\mathbf{j} = \mathbf{j}_\parallel + \mathbf{j}_\perp$. This procedure also generates effective mobility coefficients $\eta_\parallel^{\mathrm{eff}}$ and $\eta_\perp^{\mathrm{eff}}$. They can in principle be calculated from the microscopic theory by first calculating the stress tensor as a function of c and $\mathbf{p}$ and then using equations (34) and (35).

5 Conclusions

Based on an analysis of the forces acting on filaments we have developed a general framework for describing the dynamics of networks formed by polar filaments that are set into relative motion by active cross-links that induce pair-wise interactions between filaments. The work is most directly related to *in vitro* experiments on cytoskeletal filaments where molecular motors provide the active cross-links [13,16] and generalizes our work on systems in which filaments form a bundle and are aligned along a common axis [22]. Compared to the work of reference [22], the main additional feature introduced here is the effect of anisotropies in the friction of the filament in the surrounding fluid and the resulting tensorial nature of stresses. As the example treated in Section 4 shows, changes in the relative values of the respective friction coefficients can be used to switch between qualitatively different behavior.

Our work is related to earlier works where macroscopic equations were derived from microscopic rules [23–27]. These works focus largely on the aspects of pattern formation and do not address macroscopic stress tensors. Furthermore, we have not relied on the Einstein relation in our microscopic model as it is not expected to be valid far from thermodynamic equilibrium. In the present study we have restricted ourselves to the simplest case of only one kind of motors and a fixed distribution of filament lengths. Situations, when several types of motors are present or when the distribution of filament lengths is dynamic, can be treated within the same framework by appropriate modifications. This is also true if the effects of other proteins *e.g.* depolymerizing or nucleating filaments are to be taken into account.

The corresponding dynamic equations, however, quickly become rather cumbersome, such that an analysis is best carried out for the behavior on large length scales. Then coarse-graining procedures can be used that result in systems of coupled partial differential equations. As mentioned in the introduction, a different approach towards describing cytoskeletal dynamics on large length scales consists in the formulation of phenomenological continuum theories [4,8,10,11], an approach that has also been used to describe the dynamics of flocks or bacterial colonies, which share a number of similarities with motor-filament systems, see references [30,31]. These theories are based on expressions for the stress in terms of the particle density and orientational order parameters.

In the presence of filament treadmilling or motor forces $\mathbf{f}_\mathrm{m}$ which propel filaments in the fluid, interesting phenomena can occur which we have ignored here in order to keep the discussion simple. An example is the possibility of rotating flows around point defects which are associated with net torques acting on the fluid [10]. Finally, we have neglected chiral terms, which are in principle allowed since filaments are chiral objects. If interactions between filaments were chiral, the reflection symmetry which we assume would be reduced. Chiral interaction terms could also lead to the generation of torques in the system. Active chiral systems have been recently studied both experimentally and theoretically [32,33]. The role of chirality in active cellular systems provides an interesting topic for future studies.

References

1. B. Alberts *et al.*, *Molecular Biology of the Cell*, 4th ed. (Garland, New York, 2002).
2. D. Bray, *Cell Movements*, 2nd ed. (Garland, New York, 2001).
3. J. Howard, *Mechanics of Motor Proteins and the Cytoskeleton* (Sinauer Associates, Inc., Sunderland, 2001).
4. K. Kruse, J.F. Joanny, F. Jülicher, J. Prost, K. Sekimoto, Phys. Rev. Lett **92**, 078101 (2004).
5. H.Y. Lee, M. Kardar, Phys. Rev. E **64**, 056113 (2001).
6. J. Kim, Y. Park, B. Kahng, H.Y. Lee, J. Korean Phys. Soc. **42**, 162 (2003).
7. J.F. Joanny, F. Jülicher, J. Prost, Phys. Rev. Lett. **90**, 168102 (2003).
8. K. Kruse, A. Zumdieck, F. Jülicher, Europhys. Lett. **64**, 716 (2003).
9. S. Sankararaman, G.I. Menon, P.B. Kumar, Phys. Rev. E **70**, 031905 (2004).
10. K. Kruse, J.F. Joanny, F. Jülicher, J. Prost, K. Sekimoto, Eur. Phys. J. E **16**, 5 (2005).
11. A. Zumdieck, M. Cosentino Lagomarsino, C. Tanase, K. Kruse, B. Mulder, M. Dogterom, F. Jülicher, Phys. Rev. Lett. **95**, 258103 (2005).
12. K. Takiguchi, J. Biochem. **109**, 520 (1991).
13. F.J. Nédélec, T. Surrey, A.C. Maggs, S. Leibler, Nature **389**, 305 (1997).
14. T. Surrey, M.B. Elowitz, P.E. Wolf, F. Yang, F. Nédélec, K. Shokat, S. Leibler, Proc. Natl. Acad. Sci. U.S.A. **95**, 4293 (1998).
15. F.J. Nédélec, T. Surrey, A.C. Maggs, Phys. Rev. Lett. **86**, 3192 (2001).
16. T. Surrey, F. Nédélec, S. Leibler, E. Karsenti, Science **292**, 1167 (2001).
17. D. Humphrey, C. Duggan, D. Saha, D. Smith, J. Käs, Nature **416**, 413 (2002).

18. Y. Tanaka-Takiguchi, T. Kakei, A. Tanimura, A. Takagi, M. Honda, H. Hotani, K. Takiguchi, J. Mol. Biol. **341**, 467 (2004).
19. K. Sekimoto, H. Nakazawa, in *Current Topics in Physics*, edited by Y.M. Choe, J.B. Hong, C.N. Chang (World Scientific, Singapore, 1998) p. 394, physics/0004044.
20. K. Kruse, F. Jülicher, Phys. Rev. Lett. **85**, 1778 (2000).
21. K. Kruse, S. Camalet, F. Jülicher, Phys. Rev. Lett. **87**, 138101 (2001).
22. K. Kruse, F. Jülicher, Phys. Rev. E **67**, 051913 (2003).
23. T.B. Liverpool, M.C. Marchetti, Phys. Rev. Lett. **90**, 138102 (2003).
24. I.S. Aranson, L.S. Tsimring, Phys. Rev. E **71**, 050901 (2005).
25. T.B. Liverpool, M.C. Marchetti, Europhys. Lett. **69**, 846 (2005).
26. F. Ziebert, W. Zimmermann, Eur. Phys. J. E **17**, 41 (2005).
27. A. Ahmadi, T.B. Liverpool, M.C. Marchetti, Phys. Rev. E **72**, 060901 (2005).
28. M. Doi, S.F. Edwards, *The Theory of Polymer Dynamics* (Oxford University Press, New York, 1986).
29. C. Brennen, J. Mechanochem. Cell Motil. **3**, 207 (1976).
30. R.A. Simha, S. Ramaswamy, Phys. Rev.Lett. **89**, 058101 (2002).
31. J. Toner, Y. Tu, S. Ramaswamy, Ann. Phys. (N.Y.) **318**, 170 (2005).
32. I.H. Riedel, K. Kruse, J. Howard, Science **309**, 300 (2005).
33. J.-C. Tsai, F. Ye, J. Rodriguez, J.P. Gollub, T.C. Lubensky, Phys. Rev. Lett. **94**, 214301 (2005).